CONSTITUTIVE MODELS OF RUBBER ELASTICITY: A REVIEW

MARY C. BOYCE
DEPARTMENT OF MECHANICAL ENGINEERING
CENTER FOR MATERIALS SCIENCE AND ENGINEERING
MASSACHUSETTS INSTITUTE OF TECHNOLOGY
CAMBRIDGE, MA 02139

ELLEN M. ARRUDA*
DEPARTMENT OF MECHANICAL ENGINEERING
UNIVERSITY OF MICHIGAN
ANN ARBOR, MI 48109

ABSTRACT

A review of constitutive models for the finite deformation response of rubbery materials is given. Several recent and classic statistical mechanics and continuum mechanics models of incompressible rubber elasticity are discussed and compared to experimental data. A hybrid of the Flory–Erman model for low stretch deformation and the Arruda–Boyce model for large stretch deformation is shown to give an accurate, predictive description of Treloar's classical data over the entire stretch range for all deformation states. The modeling of compressibility is also addressed.

CONTENTS

I. INTRODUCTION

The macromolecular network structure of elastomeric materials enables these materials to undergo large strain, nonlinear elastic deformations. The underlying structure is essentially one of randomly oriented, long chain molecules in a network arrangement due to sparse cross-linking between the long molecules; furthermore, the intermolecular interactions are weak. The nature of this structure results in a stress–strain behavior that is primarily governed by changes in configurational entropy as the randomly-oriented molecular network becomes preferentially-oriented with stretching. The basic features of the stress–strain behavior have been well-modeled by statistical mechanics treatments of rubber elasticity (for example, see Treloar[1] for a review) as well as by invariant-based and/or stretch-based continuum mechanics theories. In the last ten years, developments in computational mechanics, specifically in finite element analysis, have enabled

* Corresponding author. Tel: 734-763-5328, fax: 734-647-3170; e-mail: arruda@umich.edu

three-dimensional, large strain analysis of complex elastomeric products to be an integral component of the design process. These developments have fueled the more critical assessment and further development of constitutive models of rubber elasticity since the need for predictive, three-dimensional models of the stress–strain behavior is a critical aspect in any numerical simulation of complex deformations. In this paper, we provide a review of constitutive models of rubber elasticity where both statistical mechanics and continuum mechanics approaches are discussed. The stress–strain responses as predicted by the various models are then compared to data as well as to one another.

II. STATISTICAL MECHANICS TREATMENTS

An excellent review of the development of statisical mechanics treatments of rubber elasticity is given in Treloar[1]; therefore, only basic aspects are provided here. The statistical mechanics approach begins by assuming a structure of randomly-oriented long molecular chains. In the Gaussian treatment[2,3] the distribution of the end-to-end length, r, of a chain is given by $P(r)$:

$$P(r) = 4\pi \left(\frac{3}{2\pi nl^2}\right)^{\frac{3}{2}} r^2 \exp\left(-\frac{3r^2}{2nl^2}\right) \tag{1}$$

where n is the number of links in the chain and l is the length of each link. The average initial chain length, L_o, is given by the root mean-square value of r:

$$L_o = \left(\overline{r^2}\right)^{\frac{1}{2}} = \left(nl^2\right)^{\frac{1}{2}} = \sqrt{n}\, l \tag{2}$$

When deformation is applied, the chain structure stretches and its configurational entropy decreases. If one considers the deformation of an assembly of N chains by a principal stretch state $(\lambda_1, \lambda_2, \lambda_3)$ and the deformation is such that the chain length r does not approach its fully extended length nl ($r \ll nl$), then the elastic strain energy function, W_G, can be derived from the change in configurational entropy and is found to be:

$$W_G = \frac{1}{2} Nk\theta(\lambda_1^2 + \lambda_2^2 + \lambda_3^2 - 3) \tag{3}$$

where k is Boltzmann's constant and θ is absolute temperature. The stress–stretch relationship is then found by differentiating the strain energy function with respect to the stretch (see Appendix).

The derivation of Equation (3) relies on r remaining significantly less than the fully extended length, nl, during the entire deformation. At large deformations, the observed stress–stretch behavior departs significantly from that predicted by the Gaussian model. At deformations where r begins to approach nl, the non-Gaussian nature of the chain stretch must be taken into account. These effects begin to be apparent at approximately $r/nl \cong .40$. Kuhn and Grün[4] accounted for the finite extensibility of chain stretch using Langevin chain statistics which account for the effect of the relative chain length, r/nl, on the configurations available to the chain. The resulting non-Gaussian force–extension relationship for a chain is given by:

$$f = \frac{k\theta}{l} \mathcal{L}^{-1}\left(\frac{r}{nl}\right) = \frac{k\theta}{l} \mathcal{L}^{-1}\left(\frac{\lambda}{\sqrt{n}}\right) \tag{4}$$

where the inverse Langevin function, $\mathcal{L}^{-1}\left(\frac{r}{nl}\right)$, is defined as follows:

$$\frac{r}{nl} = \coth\beta - \frac{1}{\beta} = \mathcal{L}(\beta) \tag{5}$$

$$\beta = \mathcal{L}^{-1}\left(\frac{r}{nl}\right) \tag{6}$$

To incorporate these more accurate individual chain statistics into a constitutive framework, it is necessary to have a model that relates the chain stretch of individual chains to the applied deformation; this is accomplished by assuming a representative network structure.

Four network models are shown in Figure 1. The unit cell used in each of these models is taken to deform in principal stretch space. The models differ in how the deformation of the chains is related to the deformation of the unit cell. We further note that the cell deformation is usually approximated to be incompressible since the bulk modulus of an elastomer is orders of magnitude larger than the shear modulus; the effects of compressibility will be discussed separately later.

In the "3-chain" model,[5] the chains are located along the axes of the initially cubic cell. The chain deforms affinely with the cell and the stretch on each chain will then correspond to a principal stretch value. The resulting strain energy function is given by:

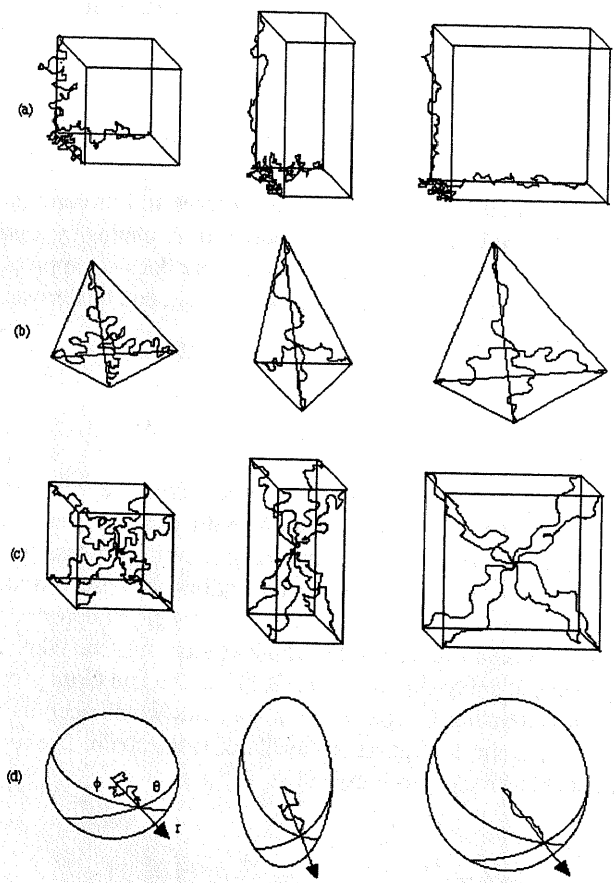

FIG. 1. — Schematic of (a) 3-chain network model, (b) 4-chain network model, (c) 8-chain network model, and (d) full network model. Each model is depicted in its undeformed state, in uniaxial tension, and in equi-biaxial tension.

$$W_{3ch} = \frac{Nk\theta}{3}\sqrt{n} \left[\lambda_1\beta_1 + \sqrt{n}\ln\left(\frac{\beta_1}{\sinh\beta_1}\right) + \lambda_2\beta_2 + \sqrt{n}\ln\left(\frac{\beta_2}{\sinh\beta_2}\right) + \lambda_3\beta_3 + \sqrt{n}\ln\left(\frac{\beta_3}{\sinh\beta_3}\right)\right] \tag{7}$$

where $\beta_i = \mathcal{L}^{-1}\left(\frac{\lambda_i}{\sqrt{n}}\right)$; for $i = 1, 2, 3$.

In the four chain tetrahedral model,[6,7] four chains are linked together at the center of a right regular tetrahedron. The tetrahedron deforms according to the imposed deformation and the chains deform accordingly with the interior junction point displacing in a non-affine manner such that equilibrium is satisified. This network structure provides a more cooperative network deformation than the 3-chain network as the chains stretch and rotate with tetrahedron deformation. Due to the non-affine displacement of the interior junction point, the relationship between the stretches of individual chains in the network to the applied stretch is a function of stretch and obtained iteratively in order to satisfy equilibrium. Therefore, a simple expression for the strain energy function in terms of applied stretches is not provided here.

In the "8-chain" model of Arruda and Boyce,[8,9] the chains are located along the diagonals of the unit cell and deform with the cell. Due to the symmetry of the chain structure, the interior junction point remains centrally located throughout the deformation and the stretch on each chain in the structure is found to be the root mean-square of the applied stretches:

$$\lambda_{\text{chain}} = \left(\frac{1}{3}(\lambda_1^2 + \lambda_2^2 + \lambda_3^2)\right)^{\frac{1}{2}} \tag{8}$$

This results in a very simple expression for the strain energy function:

$$W_{8ch} = Nk\theta\sqrt{n}\left[\beta_{\text{chain}}\lambda_{\text{chain}} + \sqrt{n}\ln\left(\frac{\beta_{\text{chain}}}{\sinh\beta_{\text{chain}}}\right)\right] \tag{9}$$

$$\beta_{\text{chain}} = \mathcal{L}^{-1}\left(\frac{\lambda_{chain}}{\sqrt{n}}\right) \tag{10}$$

In the 8-chain representation, the chains undergo tensile stretching for all imposed deformations and also rotate towards the principal axis(es) of stretch mimicking in an average sense what would be expected in the cooperative deformation of a real network.

In the full-network or total assembly of chains model,[10,11] the chains are assumed to be randomly distributed in space and to deform in an affine manner. The strain energy function is found by integrating over the stress–stretch response of all chains r in Figure 1. This integration is computationally intensive; Wu and van der Giessen have found the integration over all chains to be well approximated by a weighted average of the 3-chain and 8-chain models.

The Gaussian model and the non-Gaussian 3-chain and 8-chain network models are compared to the data of Treloar in Figures 2 through 4, respectively. The Treloar data provides the nominal stress–stretch behavior for an elastomer in uniaxial tension, pure shear, and equibiaxial tension. These data clearly show the state-of-deformation dependence of the stress–stretch behavior. All models are fit to uniaxial extension data and their predictive capability is then assessed on the shear and biaxial data. The Gaussian statistics model is found in Figure 2 to provide a reasonable model

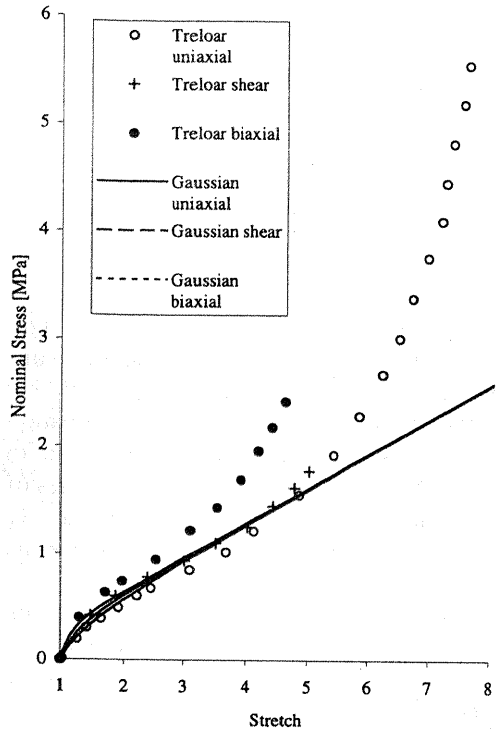

FIG. 2. — Comparison of the nominal stress–stretch behavior of the Gaussian statistics model to Treloar data in uniaxial tension, pure shear, and equibiaxial extension; $Nk\theta = .32$ MPa.

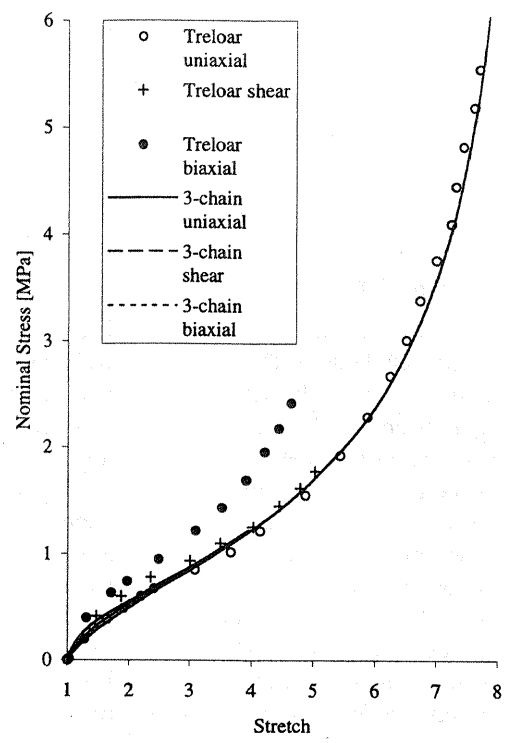

FIG. 3. — Comparison of the nominal stress–stretch behavior of the 3-chain network model to Treloar data in uniaxial tension, pure shear, and equibiaxial tension; $Nk\theta = .27$ MPa, $n = 82$.

of the stress–stretch behavior up to moderate stretches where the non-Gaussian behavior of the real material becomes evident and the model then departs significantly from the data.

The non-Gaussian 3-chain network model results are shown in Figure 3.[9] The model is found to capture the non-Gaussian nature of the stress–stretch behavior in uniaxial tension. However, although the model captures a small state-of-deformation dependence of the behavior at small stretches, it predicts nearly identical stress–stretch behavior for all deformation states at large stretches thus failing to predict the data. The 3-chain model predictions are dominated by the contribution of the chain(s) which lie along the maximum principal stretch direction(s). Therefore it does not effectively sample the network response of the underlying structure, but only the response of the chain lying along the maximum stretch direction. The 4-chain network model was found to perform better than the 3-chain model (see Arruda and Boyce[9]) since the chains deform in a more cooperative manner; however, it still fails to predict the biaxial data.

Results for the non-Gaussian 8-chain model are shown in Figure 4.[9] The 8-chain model is found to predict the significant differences between equibiaxial tension and uniaxial tension. The chains in the 8-chain network deform in a cooperative manner where the chains are found to extend with any imposed deformation and rotate toward the maximum principal stretch axis(es). The chain extensions are found to be equal to the root mean-square of the macroscopic principal stretches. This model appears to capture the effective behavior of a complicated network response in a very simple way (see Bergstrom and Boyce[12]).

The behaviors of the 3-chain, 8-chain and full-network models have been compared to uniaxial extension and biaxial extension data of James and Guth[13] in Wu and van der Giessen.[11] Each

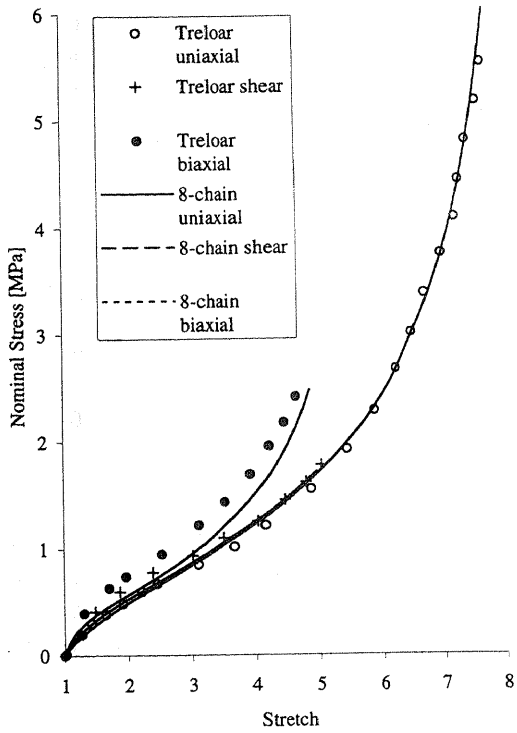

FIG. 4. — Comparison of the nominal stress–stretch behavior of the 8-chain network model to Treloar data in uniaxial tension, pure shear, and equibiaxial tension; $Nk\theta = .27$ MPa, $n = 26.5$.

model was fit to the uniaxial data and its predictive capability assessed on the biaxial data. The 3-chain model behaves in the same manner as found in the Arruda and Boyce[9] study, failing to predict the biaxial data. The 8-chain model was found to be predictive of the biaxial data and, indeed, to provide a better prediction than the full network model. The full network model predicts a biaxial stress–stretch response that falls between that predicted by the 8-chain and that predicted by the 3-chain model. The somewhat surprising lack of success of the full network model lies in its assumption of affine deformation of all chains in the non-Gaussian regime. In a real network, chains which lie along the maximum principal stretch direction would begin to stretch less with continuing deformation once they begin to approach their limiting extensibility; at that point, other chains in the network will stretch more than that predicted by affine deformation in order to accommodate the total applied stretch. Therefore, the affineness of chain deformation will be lost. The full network model assumes affine deformation of all chains and therefore, at large stretches, the contribution to the stress–stretch behavior from chains along the principal stretch direction is overestimated. We note that the 8-chain model does not assume affine deformation of all chains, but captures an effective network response.

While the models based on non-Gaussian statistics capture the effects of the limiting extensibility of the chain stretch on the stress–stretch behavior at large stretches, they do not account for discrepancies between data and Gaussian statistical mechanics models at small to moderate deformation (i.e., discrepancies when $r/nl \ll 1.0$). The departure from Gaussian theory at small to moderate stretches was first clearly highlighted in Mooney plots of data as will be discussed in more detail in the next section. There have been several modeling attempts to capture the departure of real data from the Gaussian statistics predictions at small stretches by augmenting the Gaussian

statistics model. One illustrative attempt is the constrained network model of Flory and Erman.[14] Flory and Erman[14] consider a network in which the chain junction points are constrained from a phantom characteristic via interactions with other chains. The elastic strain energy of the network is found from the sum of phantom and constraint contributions:

$$W_{FE} = W_{ph} + W_c \tag{11}$$

where W_{ph} of phantom Gaussian chains is

$$W_{ph} = \frac{1}{2}\xi k\theta(\lambda_1^2 + \lambda_2^2 + \lambda_3^2 - 3) \tag{12}$$

Note that Equation (12) differs from the Gaussian model, Equation (3), by the parameter ξ where

$$\xi = \left(1 - \frac{2}{\phi}\right)N \tag{13}$$

The parameter N is the chain density and ϕ is the number of chains meeting at a junction. When $\phi = 4$ the junction is tetrafunctional and the strain energy of the phantom network in Equation (12) is one-half of the Gaussian strain energy in Equation (3). The contribution of constraints to the strain energy is given as:

$$W_c = \frac{1}{2}Nk\theta \sum_i [B_i + D_i - \ln(B_i + 1) - \ln(D_i + 1)] \tag{14}$$

where

$$B_i = \kappa^2(\lambda_i^2 - 1)(\lambda_i^2 + \kappa)^{-2} \tag{15}$$

$$D_i = \lambda_i^2 \kappa^{-1} B_i \tag{16}$$

and where κ is a measure of the strengths of the constraints which depends on the relative sizes of free (phantom) fluctuations and actual constrained fluctuations. This constrained network model depends on the parameters N, ϕ, and κ. In it $\kappa \to \infty$ for completely constrained junctions and $\kappa \to 0$ in the phantom chain limit; N can take on any large positive value and ϕ must be greater than two.

The Flory and Erman model is compared to Treloar's data in Figure 5. For the Flory and Erman model the network is assumed to be tetrafunctional and $\phi = 4$ is used. If the Flory and Erman model were to be simulated with the same value of N as was used in the Gaussian simulations of Figure 2 the response would approach one-half of the Gaussian response as $\kappa \to 0$. Here the best overall fit to the data is sought in the small stretch regime to illustrate the utility of the Flory and Erman model in capturing the precise shape of the initial nominal stress versus stretch response, Figure 5(a). The parameters chosen for uniaxial tension are used in the prediction of the equibiaxial response. The Flory and Erman model predicts the small stretch response in equibiaxial extension quite well. In Figure 5(b) we see that at large stretches the Flory and Erman model deviates markedly from the actual response as the Gaussian statistics reach the limit of their applicability, thereby highlighting the need for non-Gaussian terms in the strain energy function. Indeed, the combination of the highly

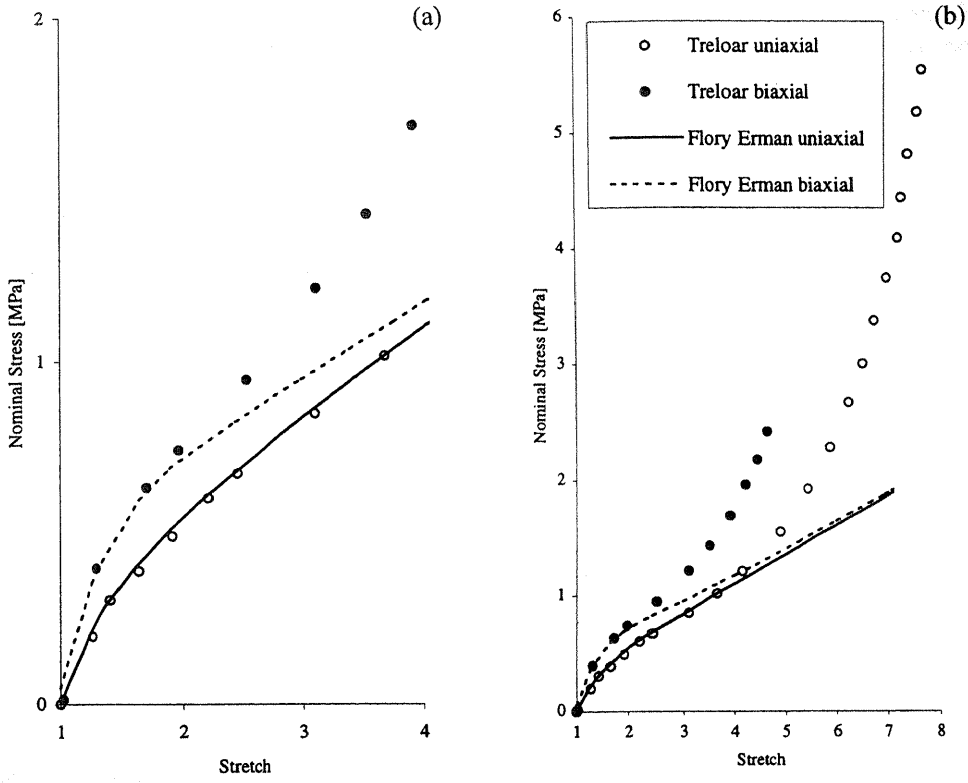

FIG. 5. — Comparison of the nominal stress–stretch behavior of the Flory–Erman constrained chain model to the Treloar data. Flory–Erman: $Nk\theta = .68$ MPa, $\phi = 4$, $\kappa = .55$.

tailorable Flory and Erman model for small stretches with the eight chain model for the large stretch response and deformation state dependence would be expected to describe the data over the entire extensibility range in a more precise manner than any of the models presented. Figure 6 examines the result of replacing the phantom strain energy in Equation (11) with the non-Gaussian eight chain strain energy of Equation (9). The equibiaxial prediction is improved especially in the small stretch region.

III. INVARIANT-BASED CONTINUUM MECHANICS TREATMENTS

Most continuum mechanics treatments of rubber elasticity begin with the fundamental basis of continuum mechanics for an isotropic, hyperelastic material which is that the strain energy density must depend on stretch via one or more of the three invariants, I_i, of the stretch tensor:

$$\begin{aligned} I_1 &= \lambda_1^2 + \lambda_2^2 + \lambda_3^2 \\ I_2 &= \lambda_1^2\lambda_2^2 + \lambda_2^2\lambda_3^2 + \lambda_1^2\lambda_3^2 \\ I_3 &= \lambda_1^2\lambda_2^2\lambda_3^2 \end{aligned} \tag{17}$$

As indicated earlier, the elastomer is often approximated to be incompressible; thus I_3 is taken to be constant and equal to 1.0 and does not contribute to the strain energy. As proposed by Rivlin,[15] one general representation of W is given by,

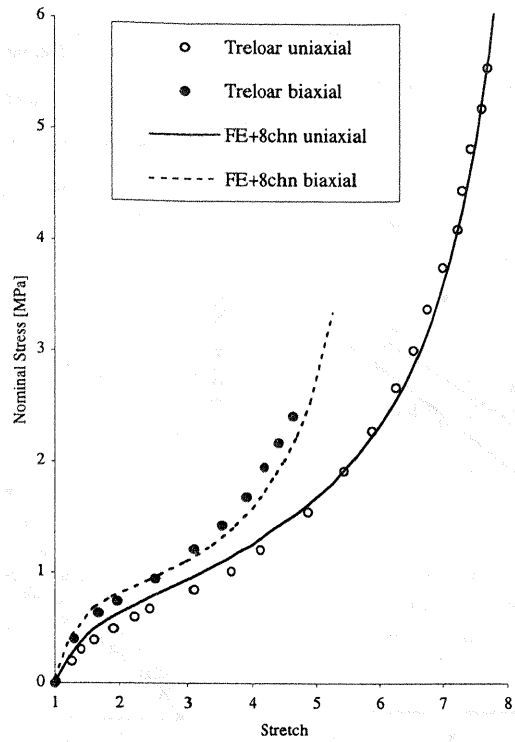

FIG. 6. — Comparison of the nominal stress–stretch behavior of the combined Flory and Erman constraints and the eight chain model to the Treloar data.

$$W_R = \sum_{i,j=0}^{\infty} C_{ij}(I_1 - 3)^i (I_2 - 3)^j \tag{18}$$

where C_{ij} are material parameters. When only the first term is retained, one obtains,

$$W_{NH} = C_{10}(I_1 - 3) \tag{19}$$

which is often called the neo-Hookean model. Note that Equation (19) is the continuum mechanics equivalent to the Gaussian model presented in Equation (3) where $C_{10} = \frac{1}{2}Nk\theta$.

By keeping the second term of the Rivlin expression, the equation first derived by Mooney[16] is obtained:

$$W_{MR} = C_{10}(I_1 - 3) + C_{01}(I_2 - 3) \tag{20}$$

This model is often referred to as the Mooney–Rivlin model and has been extensively utilized in studies of elastomer deformation. Mooney arrived at Equation (20) by determining an expression for the strain energy that would provide a constant modulus in shear (a modulus that did not depend on the shear strain). The popularity of the Mooney–Rivlin model is perhaps due to its apparent success in capturing deviations from the Gaussian/neo-Hookean model in uniaxial tension as demonstrated in Mooney plots.

A Mooney plot is an alternative method for plotting the nominal stress–stretch behavior. For uniaxial loading (tension or compression) the nominal stress (f)–stretch (λ) behavior for the neo-Hookean/Gaussian model is given by:

$$f = 2C_{10}(\lambda - \frac{1}{\lambda^2}) \tag{21}$$

and, for the Mooney–Rivlin model, is given by:

$$f = 2(C_{10} + \frac{C_{01}}{\lambda})(\lambda - \frac{1}{\lambda^2}) \tag{22}$$

A Mooney plot graphs the quantity of reduced stress $f/(\lambda - \frac{1}{\lambda^2})$ as a function of $(1/\lambda)$. A material obeying Gaussian statistics would appear as a straight line of zero slope on a Mooney plot. Several investigators have shown that plotting uniaxial tension data on a Mooney plot yields a straight line of non-zero slope in the small to moderate stretch range thus supporting the Mooney–Rivlin model.[1,15,17,18] (It is also interesting to note that the slope of the linear regime decreases with swelling. This decrease suggests that the deviation from Gaussian behavior is due to interactions or constraints of neighboring chains, consistent with the Flory–Erman introduction of a strain energy term associated with network constraint. Also, the stretch at which the Mooney plot becomes nonlinear [i.e., exhibits an upturn] is found to decrease with swelling, consistent with the non-Gaussian aspect of chain stretch.) Figure 7 depicts the Mooney plot for the uniaxial tension data of several rubber materials showing the linear behavior at small to moderate tensile stretches ($.5 < \frac{1}{\lambda} < 1$) and the "up-turn" at larger stretches ($\frac{1}{\lambda} < .5$) indicating the non-Gaussian regime. The rubber materials in Figure 7 include (1) Mullins' data[19] on five rubbers (a–e) with varying crosslink density where each shows the linear behavior followed by the up-turn and illustrate that the up-turn occurs earlier for the more highly crosslinked materials; (2) the Treloar tension data (f) presented in the earlier stress–stretch plots which also show the nearly linear behavior at small stretches and the up-turn in the Mooney plot at large stretches; and (3) Rivlin and Saunders data (g)[20] for a rubber in tension as well as in compression. We note that the Rivlin and Saunders data

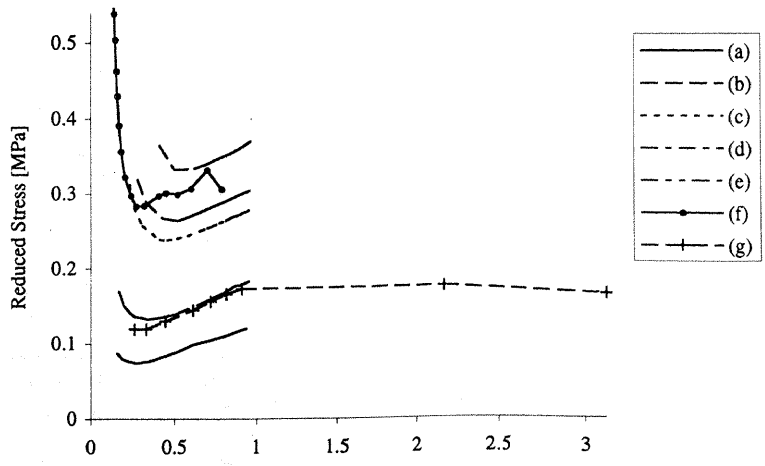

FIG. 7. — Mooney plot of uniaxial tension force extension data of five elastomers of increasing crosslink density from (a) to (e).[19] Curve (f) data are from Treolar[3] and curve (g) data are from Rivlin and Saunders.[20] Reprinted from L. Mullins, *J. Appl. Polym. Sci.* **2**, 257 (1959) by permission of John Wiley & Sons, Inc.

show that the linear behavior observed in the Mooney plot tensile data is not sustained as one goes from tension to compression. More recently, it has been shown (see, for example, Arruda and Boyce[8,9]) that the Mooney–Rivlin model can potentially grossly overestimate stresses at moderate to large deformations in different deformation states, further highlighting the deficiences of this model.

Figure 8 depicts the stress–stretch behavior of the Mooney–Rivlin model compared to the Treloar data. A best fit to the uniaxial tension data results in a far too stiff prediction of the biaxial data even with a C_{01} coefficient one-order of magnitude lower than the C_{10} coefficient as is typical in Mooney–Rivlin fits. The gross errors arise due to the high values of I_2 in biaxial stretching states (such as occur in biaxial tension or uniaxial compression). Indeed, Rivlin and Saunders[20] suggested that C_{01} should not be constant, but should be dependent on I_2, decreasing with increasing I_2.

Working within the continuum mechanics framework for the strain energy function as proposed by Rivlin, Equation (18), several investigators have used higher order terms in I_1 and, in some cases, I_2, to account for the departure from neo-Hookean/Gaussian behavior at large stretches. One model of this type is the Yeoh model[21]:

$$W_Y = C_{10}(I_1 - 3) + C_{20}(I_1 - 3)^2 + C_{30}(I_1 - 3)^3 \tag{23}$$

Using the higher order I_1 terms in the strain energy function has been shown to work well in capturing different deformation states at moderate to large deformations. An alternate high order I_1 model has recently been proposed by Gent[22] and takes the form:

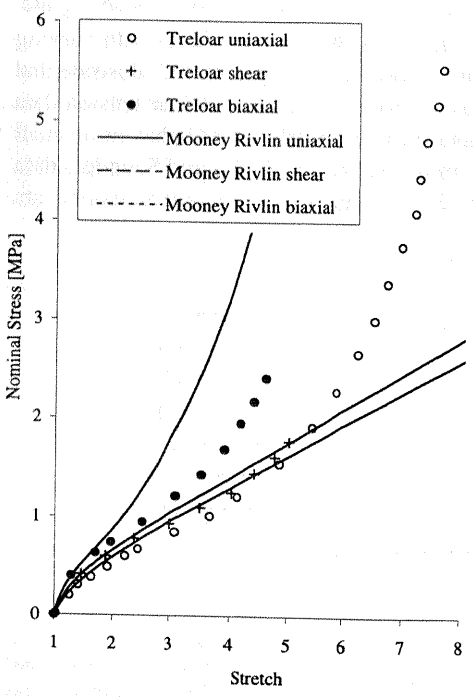

FIG. 8. — Comparison of the nominal stress–stretch behavior of the Mooney–Rivlin model to the Treloar data in uniaxial tension, simple shear, and equi-biaxial tension; C_{10} = .16 MPa, C_{01} = 0.015 MPa.

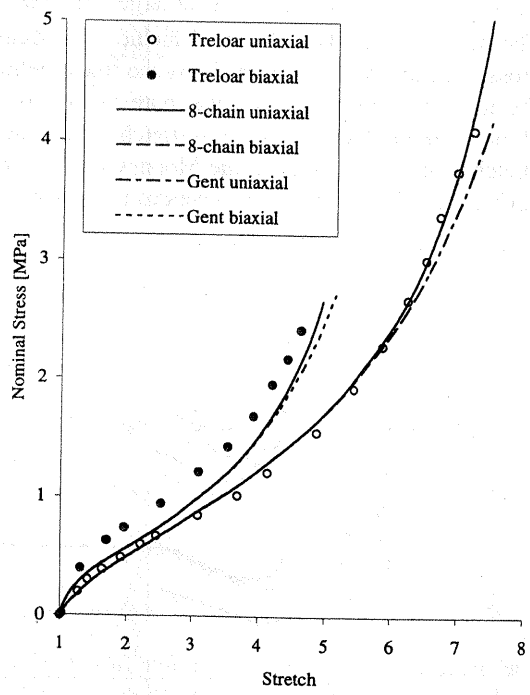

FIG. 9. — The Gent model and the Arruda–Boyce 8-chain model compared to one another and to Treloar data in uniaxial tension and equi-biaxial tension; Gent: E = .81 MPa, J_m = 101.

$$W_{\text{Gent}} = -\frac{E}{6}\ln\left[1 - \frac{J_1}{J_M}\right] \tag{24}$$

where $J_1 = (I_1 - 3)$, E is the small strain tensile modulus, and J_M denotes a maximum value for J_1 where as J_1 approaches J_M the material approaches limiting extensibility. As discussed in Boyce,[23] the natural logarithm term in the Gent model can be expanded to yield the following expression for the strain energy:

$$W_{\text{Gent}} = \frac{E}{6}\left[(I_1 - 3) + \frac{1}{2J_M}(I_1 - 3)^2 + \frac{1}{3J_M^2}(I_1 - 3)^3 + \cdots + \frac{1}{(n+1)J_M^n}(I_1 - 3)^{n+1}\right] \tag{25}$$

which is a form of the Rivlin expression, Equation (18), with all coefficients, C_{i0}, now related to the two properties E and J_M.

Indeed, as discussed in Arruda and Boyce,[8,9] it is interesting to observe that the strain energy expression for the 8-chain model, Equation (9), is I_1-based since it is a function of chain stretch, λ_{chain}, which is equivalent to $\sqrt{I_1/3}$. Equation (9) can be expanded to polynomial form to give:

$$W_{8ch} = NK\theta\left[\frac{1}{2}(I_1 - 3) + \frac{1}{20n}(I_1^2 - 9) + \frac{11}{1050n^2}(I_1^3 - 27) + \frac{19}{7000n^3}(I_1^4 - 81) + \frac{519}{673750n^4}(I_1^5 - 243) + \cdots\right] \tag{26}$$

which can be re-written in a general invariant-based form as:

$$W = \sum_{i=1}^{n} C_i(I_1^i - 3^i) \tag{27}$$

where the C_i are all determined *a priori* as functions of the material properties n and N. Boyce[23] showed how the Gent model, Equations (24) and (25), is essentially equivalent to the 8-chain model. Figure 9 depicts the predictions of the Arruda–Boyce and the Gent models compared to Treloar data; both models were fit to the uniaxial tension data and the biaxial tension model results are predictions. The Treloar data and model predictions are presented at small and moderate stretches to highlight the model similarities. The models are shown to provide similar results and both are found to be predictive.

Therefore, the success of the higher order I_1 continuum mechanics models is due to their mimicking the physics of successful non-Gaussian statistics models thus providing the connection between the higher order continuum models and the statistical mechanics models (similar to the neo-Hookean model being equivalent to the Gaussian model).

One caution regarding the use of phenomenological higher order I_1 continuum mechanics models is that the constants chosen must result in physically realistic and stable constitutive responses in all deformation states. The Drucker stability criterion requires that the tangential stiffness matrix (or Hessian) be positive definite.[24] The Hessian may be written in terms of the strain energy density as:

$$H_{ijkl} = \frac{\partial^2 W}{\partial\varepsilon_{ij}\partial\varepsilon_{kl}} \tag{28}$$

where ε_{ij} is the strain. One judicious choice for stable model constants would be to choose all coefficients to be positive-valued. Johnson et al.[25] showed that for a third-order Rivlin polynomial strain energy function the coefficients must be positive-valued for Drucker stability to be achieved. Such a choice may be overly restrictive in some continuum mechanics models. Przybylo and Arruda[26] recently demonstrated that restricting coefficients to be stable in higher order I_1 models reduces the quality of the fit to experimental data. The constants in the statistical mechanics models and the model of Gent are unconditionally stable.

IV. STRETCH-BASED CONTINUUM MECHANICS TREATMENTS

Strain energy density functions based on the principal stretches as opposed to the stretch invariants have also been proposed by several investigators. Valanis and Landel[27] proposed a model whereby the strain energy is a separable function of the principal stretches:

$$W_{VL} = \sum_{i=1}^{3} w(\lambda_i) \tag{29}$$

The three functions $w(\lambda_i)$ are all of the same form although a specific analytic expression for the form of the $w(\lambda_i)$ was not given. The model did not contain adjustable parameters per se. The functions $w(\lambda_i)$ are experimentally obtained. Biaxial tests in which one stretch is held constant while another is varied are used to experimentally characterize the data as $(\lambda_i, w(\lambda_i))$ pairs for λ_j = constant, $j \neq i$.

Following a similar approach, Ogden[28] proposed a specific form for the strain energy function in terms of principal stretches:

$$W_o = \sum_n \frac{\mu_n}{\alpha_n} \left(\lambda_1^{\alpha_n} + \lambda_2^{\alpha_n} + \lambda_3^{\alpha_n} - 3\right) \tag{30}$$

in which the μ_n and α_n are constants and may have any value including non-integer values. The degree of the sum may be adjusted as needed to fit the data at hand. The model easily lends itself to be tailored in this manner; reasonable fits to data have been achieved by Ogden[28] for $n \geq 3$ in which case the minimum number of independently adjustable parameters is six. Twizell and Ogden[29] consider stability of Equation (30) which leads to $\mu_n \alpha_n > 0$ for all n. They use a Levenberg–Marquardt non-linear least squares optimization algorithm to find stable constants for $n = 3$ and $n = 4$ and find improved fits to data as n increases. Przybylo and Arruda[26] show for $n = 1$ and $n = 2$ the quality of fit to experimental data is reduced when the constants are restricted by stability considerations.

V. EFFECTS OF COMPRESSIBILITY

Although rubber elastic materials are generally considered to be incompressible, in reality they are only nearly incompressible, and the most accurate constitutive models will include compressibility. A practical application for rubber elastic constitutive models is their implementation into finite element codes to simulate complex deformations. A compressible material model helps to avoid the numerical problems inherent in incompressible formulations. There are also numerous elastomeric products that perform under confined conditions where the bulk response is important.

Compressible forms of the strain energy function W have traditionally been developed in one of two ways (see, for example, Ogden,[30] Fried and Johnson,[31] and, more recently, Anand.[32]) Both begin by removing the incompressibility restriction that $J = 1$ where J is the volume ratio,

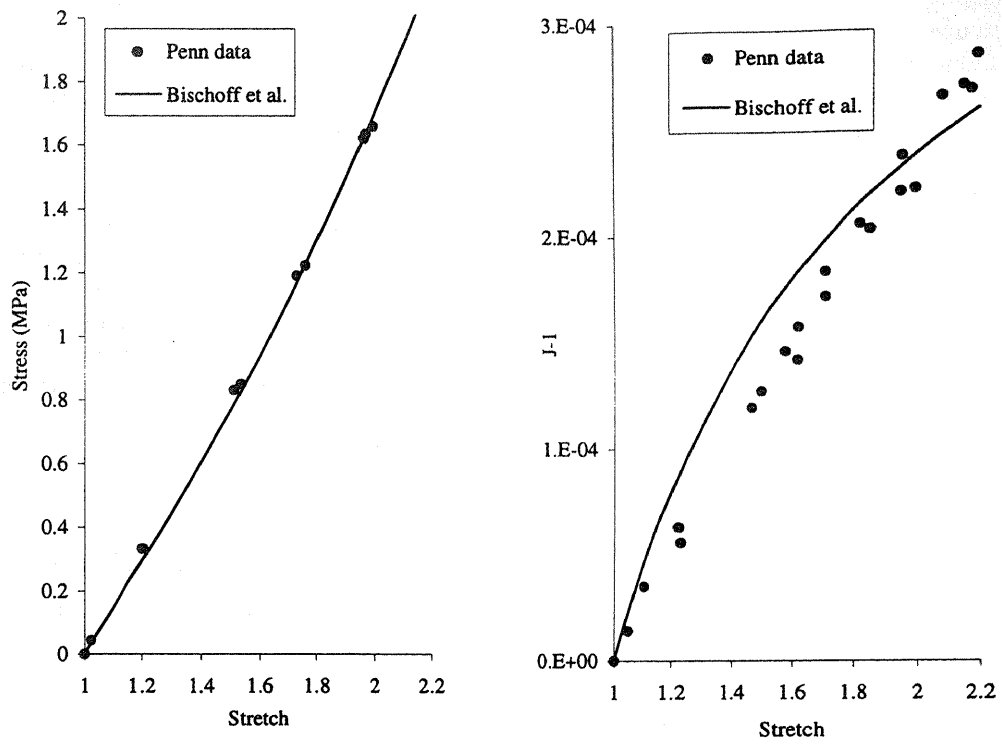

FIG. 10. — Uniaxial stress versus stretch and volume change versus stretch data from Penn,[33] and corresponding fit using Equations (33) and (34) with $n = 40$, $Nk\theta = .47$ MPa, $B = 1.0 \times 10^3$ MPa, and $\alpha = 4$.

$J = \sqrt{I_3}$. One approach assumes the strain energy is a separable function of a deviatoric strain energy and a hydrostatic strain energy.

$$W = W_D(\bar{I}_1, \bar{I}_2) + W_H(J) \tag{31}$$

where $\bar{I}_1$ and $\bar{I}_2$ are invariants of the deviatoric stretch tensor, $\bar{I}_1 = J^{-2/3} I_1$, $\bar{I}_2 = J^{-4/3} I_2$. Other compressible formulations append a bulk strain energy term to an existing strain energy form,

$$W = W_a(I_1, I_2, J) + W_b(J) \tag{32}$$

In this formulation both terms on the right side of the equation contain contributions due to the volume change. The second term of both Equation (31) and (32) is considered to arise due to changes in internal energy whereas the first term arises from changes in configurational entropy. It is the second term in Equation (32) that captures the very stiff nature of the bulk modulus when compared to the shear modulus.

Penn[33] argued that a compressible strain energy function of the form Equation (31) cannot qualitatively capture experimental data from both hydrostatic and uniaxial tension experiments, even at small deformations. Recently Ehlers and Eipper[34] echoed Penn's conclusion by examining the transverse deformations predicted by models of the type, Equation (31), and finding them to be unphysical at large deformations. Compressible model development would benefit from data

exploring the volume changes on deformation, however, very little experimental data exist in the literature.

Dilatometer tests were used by Penn[33] to measure volume change during uniaxial extension. These data are available for relatively small deformations and are reproduced in Figure 10 as stress and volume change versus stretch. The volume change is observed to increase at a decreasing rate with continued uniaxial deformation.

Pressure versus volume data during hydrostatic compression tests have been obtained by Adams and Gibson,[35] and by Bridgman.[36] Both groups obtained these data by placing specimens in a fluid bath inside a cylinder and piston apparatus and pressurizing the cylinder by displacing the piston. The experimental results appear in Figure 11. For relatively large hydrostatic deformations ($J = .8$), the pressure versus volume change response of elastomers is seen to be highly non-linear indicating that a $W_H(J)$ type term in an equation of the form of Equation (32) would be nonlinear in J.

Recently Bischoff et al.[37] proposed a compressible model based on the 8-chain strain energy function that follows the form of Equation (32),

$$W = Nk\theta\sqrt{n}\left[\beta_{\text{chain}}\lambda_{\text{chain}} + \sqrt{n}\ln\left(\frac{\beta_{\text{chain}}}{\sinh\beta_{\text{chain}}}\right) + \frac{\beta_o}{3}ln\left(\frac{1}{J}\right)\right] + W_b(J) \qquad (33)$$

where $\beta_o = \mathcal{L}^{-1}\{1/\sqrt{n}\}$. Bischoff et al.[37] show that additional restrictions owing to stability and physically realistic volume changes (see Ogden[38] for a discussion of these) result in a complicated form for $W_b(J)$. They examine the form

$$W_b(J) = \frac{B}{\alpha^2}\{\cosh[\alpha(J-1)] - 1\} \qquad (34)$$

which satisfies all restrictions on the compressibility and gives a bulk modulus at $\lambda_1 = 1$ of $B + 2\frac{Nk\theta}{3}$. Thus B must be much larger than the rubbery modulus, $\frac{Nk\theta}{3}$. The constant α is adjusted to fit data of the type in Figures 10 and 11.

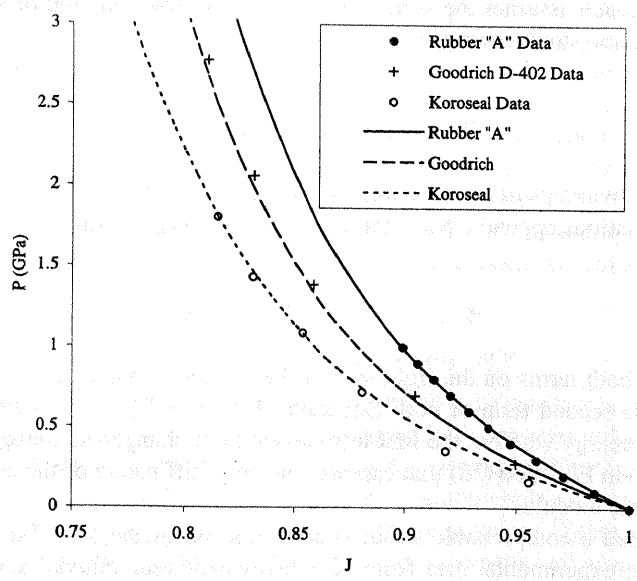

FIG. 11. — Hydrostatic compression data for materials Koroseal®and Goodrich D-402 reproduced from Bridgman[36] and rubber "A" reproduced from Adams and Gibson.[35] Equation (33): $n = 20$ and $Nk\theta = .411$ kPa for all three materials. Equation (34): rubber "A", $B = 7.2$ GPa, $\alpha = 14$; Goodrich, $B = 5.3$ GPa, $\alpha = 14$; and Koroseal, $B = 4.3$ GPa, $\alpha = 13$.

This model is compared to the experimental volume versus deformation data in Figures 10 and 11. In Figure 10 stress and volume are plotted versus uniaxial stretch with model predictions using stress derived from Equations (33) and (34) (see Appendix). In Figure 11 the hydrostatic stress versus volume ratio simulations are plotted for three materials along with the data of Adams and Gibson[35] and of Bridgman.[36] The model is capable of accurate description of the entire non-linear pressure versus volume response of rubber materials in hydrostatic compression as well as the volume change and stress during uniaxial tension. The Bischoff et al.[37] non-linear energetic compressibility function model is compared in Figure 12 to a linear energetic compressibility function

$$W_b(J) = \frac{B}{2}(J-1)^2 \tag{35}$$

that contributes $B(J-1)$ to the pressure in a hydrostatic test. Both energetic compressibility functions are shown against the hydrostatic Goodrich D-402 data from Figure 11. Nonlinearity in the compressibility is clearly needed at finite volume changes which the Bischoff et al.[37] model provides.

In the Gaussian range Equation (33) reduces to

$$W = \frac{Nk\theta}{2}(\lambda_1{}^2 + \lambda_2{}^2 + \lambda_3{}^2 - 3) + Nk\theta \ln\left(\frac{1}{J}\right) + W_b(J) \tag{36}$$

which is the Gaussian strain energy of Equation (3) plus additional compressibility terms from entropy considerations ($Nk\theta \ln(1/J)$) and internal energy considerations ($W_b(J)$). It is shown in Bischoff et al.[37] that the $Nk\theta \ln \frac{1}{J}$ term is entropic in origin and may be derived by including volume changes in the classical Gaussian treatment. As discussed earlier, volume changes have been traditionally neglected in the configurational entropy calculation leading to Equation (3) (see, for example, Treloar[1]), although Wall and Flory[39] and Flory[40,41] have previously reported a similar entropic term.

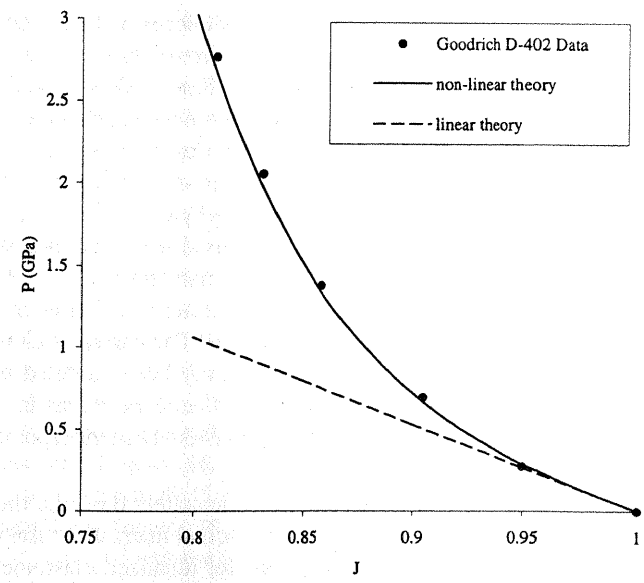

FIG. 12. — Hydrostatic compression data for Goodrich D-402 reproduced from Bridgman[36] versus non-linear and linear energetic compressibility functions. The non-linear model constants used above are the same as those used previously in Figure 11. Linear: $B = 5.3$ GPa.

VI. CONCLUSIONS

The constitutive modeling of the stress–strain behavior of rubber elastic materials has been reviewed. It has been found that developments in statistical mechanics approaches have enabled predictive modeling of the three-dimensional stress–stretch response of elastomers. Statistical mechanics models which account for the non-Gaussian nature of the molecular chain stretch together with an effective or representative network structure such as the Arruda–Boyce 8-chain model appear to provide the most predictive model of the larger strain behavior under different states of deformation. Furthermore, the physically based foundation of the non-Gaussian statistical mechanics network models provides a constitutive law that requires only two material properties—the network chain density, N, which is determined from the small strain behavior, and the limiting chain extensibility, $\sqrt{n}$, which is determined from the behavior at large strain. Inclusion of network constraint effects as proposed in the Flory–Erman model provides further improvements to model predictions at small strains.

The continuum mechanics invariant-based constitutive models were found to be equivalent phenomenological representations of the microstructurally based statistical mechanics models. In particular, the role of the first and second invariants of the stretch tensor were detailed. The first invariant, I_1, is found to correlate with the average chain stretch in the network model. Strain energy expressions which contain a polynomial series in I_1 including higher order I_1 terms are, in effect, capturing the non-Gaussian nature of the network stretch behavior. Strain energy expressions which contain the second invariant of stretch, I_2, should be used with caution; forms such as the Mooney–Rivlin model are found to be overly stiff in certain types of deformation. Generalized polynomial strain energy models containing higher order I_1 and I_2 terms are popular in commercial finite element codes for example because they offer the option of automatic data fitting. Caution is advised whenever a phenomenological model is fit to data because the best fits may be achieved with unstable constants. Precise fits are indeed possible with some of the continuum mechanics constitutive models but such precision comes at the expense of increased model complexity viz. the many constants and data sets required.

Statistical mechanics models offer predictive capabilities with a minimal number of material parameters that have a physical connection to the molecular microstructure. The stability of these constants is never an issue in data fitting. The success of the microstructurally-based statistical mechanics models has provided a foundation for extending these models to predict other complex phenomena. For instance the optical properties of elastomers have been examined by incorporating the additional physics associated with the optical anisotropy or birefringence of an elastomer with the molecular polarizability anisotropy (see Treloar,[1] Arruda and Przybylo,[42] Wu and van der Giessen,[43] and von Lockette and Arruda[44]). Arruda and Przybylo[42] recently developed a network polarizability tensor for the 8-chain model geometry and used it to predict elastomeric network birefringence. von Lockette and Arruda[44] computed the Raman tensor for the 8-chain model and demonstrated its ability to predict optical anisotropy using either retardation or Raman scattering data during homogeneous and inhomogeneous deformations. The current technologically important problem of hysteresis in elastomeric systems has recently been modeled by Bergstrom and Boyce[45,46] using statistical mechanics models of loose and network chains in an 8-chain model geometry. Effects of filler particles such as carbon black have also been incorporated into statistical mechanics models.[46–48]

The network models from statistical mechanics can adequately describe the deformation response of random elastomers by effectively averaging the actual microstructural response via simplifying assumptions. The validity of these assumptions for idealized elastomer microstructures has recently been examined using molecular level simulations.[12,49] Results of these simulations have been used in turn to refine the statistical mechanics models of idealized networks.[50] Molecular simulations of unimodal[12,49] and bimodal[50] networks via Monte Carlo techniques show the initial

chain lengths in crosslinked networks to be very near the root mean-square length assumed in Gaussian and non-Gaussian statistical mechanics models. Bergstrom and Boyce[12] show that upon deformation of a unimodal network the mean chain stretch and angle follow the 8-chain model prediction, Equation (8). Molecular crosslinking simulations of bimodal networks by von Lockette and Arruda[49] demonstrate that the short chains in bimodal networks are initially below their root mean-square length. This result has led to a new network model for bimodal elastomers that is predictive of the stress and optical response changes with bimodal network composition.[50]

Finally, the effects of compressibility are important in certain applications and can be modeled by appropriate extension of the strain energy expression. Volumetric deformation is found to have a modest effect on the entropic contribution to the strain energy density and, more importantly, to add internal energy contributions to the strain energy density. Although data are scarce, the data that do exist show there to be a nonlinear relationship between pressure and volumetric strain. This effect has been well-modeled by Bischoff et al.[37] by including a nonlinear volumetric term in the strain energy function.

VII. ACKNOWLEDGEMENTS

M. C. Boyce acknowledges support from the US NSF Grant No. CMS-9622526 and the NSF MRSEC MIT CMSE through Grant No. DMR-98-08941. E. M. Arruda acknowledges support from the US NSF Grant No. CMS-035812. We thank Dr. Perry Marteny of The Goodyear Tire & Rubber Company and *Rubber Chemistry and Technology* for suggesting this review paper.

VIII. REFERENCES

[1]L. R. G. Treloar, "The Physics of Rubber Elasticity," Oxford University Press, 1975.

[2]F. T. Wall, *J. Chem. Phys.* **10,** 485 (1942).

[3]L. R. G. Treloar, *Trans. Faraday Soc.* **40,** 59 (1944).

[4]W. Kuhn and F. Grühn, *Z. Kolloid* **101,** 248 (1942).

[5]M. Wang and E. Guth, *J. Chem. Phys.* **20,** 1144 (1952).

[6]P. J. Flory and J. Rehner Jr., *J. Chem. Phys.* **11,** 512 (1943).

[7]L. R. G. Treloar, *Trans. Faraday Soc.* **42,** 83 (1946).

[8]E. M. Arruda and M. C. Boyce, MIT Internal Report, available through M. C. Boyce, 1991.

[9]E. M. Arruda and M. C. Boyce *J. Mech. Phys. Solids* **41,** 389 (1993).

[10]L. R. G. Treloar, *Trans. Faraday Soc.* **50,** 881 (1975).

[11]P. D. Wu and E. van der Giessen, *J. Mech. Phys. of Solids* **41,** 427 (1993).

[12]J. S. Bergstrom and M. C. Boyce, to be submitted to —Macromolecules (2000).

[13]H. M. James and E. Guth, *J. Chem. Phys.* **11,** 455 (1943).

[14]P. J. Flory and B. Erman, *Macromolecules* **15,** 800 (1982).

[15]R. S. Rivlin, *Philos. Trans. R. Soc. London, Ser. A* **241,** 379 (1948).

[16]M. J. Mooney, *J. Appl. Phys.* **11,** 582 (1940).

[17]S. M. Gumbrell, L. J. Mullins, and R. S. Rivlin, *Trans. Faraday Soc.* **49,** 1495 (1953).

[18]M. C. Morris, *J. Appl. Polym. Sci.* **8,** 545 (1964).

[19]L. Mullins, *J. Appl. Polym. Sci.* **2,** 257 (1959).

[20]R. S. Rivlin and D. W. Saunders, *Philos. Trans. Roy. Soc. London, Ser. A* **243,** 251 (1951).

[21]O. H. Yeoh, RUBBER CHEM. TECHNOL. **66,** 754 (1993).

[22]A. Gent, RUBBER CHEM. TECHNOL. **69,** 59 (1996).

[23]M. C. Boyce, RUBBER CHEM. TECHNOL. **69,** 781 (1996).

[24]W. F. Chen and A. T. Saleeb, "Constitutive Equations for Engineering Materials," Elsevier, New York, 1982.

[25]A. R. Johnson, C. J. Quigley, and J. L. Mead, RUBBER CHEM. TECHNOL. **67,** 904 (1994).

[26]P. A. Przybylo and E. M. Arruda, RUBBER CHEM. TECHNOL. **71,** 730 (1998).

[27]K. C. Valanis and R. F. Landel, *J. Appl. Phys.* **38,** 2997 (1967).

[28]R. W. Ogden, *Proc. R. Soc. London, Ser. A* **326,** 565 (1972).
[29]E. H. Twizell and R. W. Ogden, *J. Austral. Math. Soc. Ser. B* **24,** 424 (1983).
[30]R. W. Ogden, *J. Mech. Phys. Solids* **24,** 323 (1976).
[31]I. Fried and A. R. Johnson, *Comput. Meth. Appl. Mech. Eng.* **69,** 53 (1988).
[32]L. Anand, *Comput. Mech.* **18,** 339 (1996).
[33]R. W. Penn, *Trans. Soc. Rheol.* **14(4),** 509 (1970).
[34]W. Ehlers and G. Eipper, *Acta Mech.* **130,** 17 (1998).
[35]L. H. Adams and R. E. Gibson, *J. Acad. Sci. Wash.* **20,** 213 (1930).
[36]P. W. Bridgman, *Proc. Am. Acad. Arts Sci.* **76,** 9 (1944).
[37]J. E. Bischoff, E. M. Arruda, and K. Grosh, submitted to RUBBER CHEM. TECHNOL. (2000).
[38]R. W. Ogden, *Proc. R. Soc. London, Ser. A* **328,** 567 (1972).
[39]F. T. Wall and P. S. Flory, *J. Chem. Phys.* **19,** 1435 (1951).
[40]P. J. Flory, *Trans. Faraday Soc.* **57,** 829 (1961).
[41]P. J. Flory, *Proc. R. Soc. London, Ser. A* **351,** 351 (1976).
[42]E. M. Arruda and P. Przybylo, *Polym. Eng. Sci.* **35,** 395 (1995).
[43]P. D. Wu and E. van der Giessen, *Philos. Mag., Ser. A* **71,** 1191 (1995).
[44]P. R. von Lockette and E. M. Arruda, *Acta Mechanica* **134,** 81 (1999).
[45]J. S. Bergstrom and M. C. Boyce, *J. Mech. Phys. Solids* **46,** 931 (1998).
[46]J. S. Bergstrom and M. C. Boyce, submitted to *Mechan. Mater.* (1999).
[47]S. Govindjee and J. C. Simo, *J. Mech. Phys. Solids* **39,** 112 (1991).
[48]J. S. Bergstrom and M. C. Boyce, RUBBER CHEM. TECHNOL. **72,** 633 (1999).
[49]P. R. von Lockette and E. M. Arruda, submitted to —Macromolecules (2000).
[50]P. R. von Lockette and E. M. Arruda, submitted to *J. Comp. Poly. Sci.* (2000).

[*Received February 19, 2000; revised March 14, 2000*]

IX. APPENDIX

When the constitutive relationship is expressed in terms of the strain energy density function, W, the stress–stretch behavior is found by differentation with respect to the stretch. For the case of incompressibility, the principal Cauchy (true) stresses, σ_i are found by differentiating with respect to the principal stretches, λ_i:

$$\sigma_i = \lambda_i \frac{\partial W}{\partial \lambda_i} + p \quad \text{(no sum on } i\text{)} \tag{A1}$$

where p is the pressure determined by satisfying boundary conditions. If $\hat{W} = W(I_1, I_2)$, this may be written as:

$$\sigma_i = \lambda_i \left[\frac{\partial W}{\partial I_1} \frac{\partial I_1}{\partial \lambda_i} + \frac{\partial W}{\partial I_2} \frac{\partial I_2}{\partial \lambda_i} \right] + p \quad \text{(no sum on } i\text{)} \tag{A2}$$

The corresponding nominal stress is given by:

$$f_i = \frac{1}{\lambda_i} \sigma_i \quad \text{(no sum on } i\text{)} \tag{A3}$$

For the case of the compressible material, the bulk behavior must also be considered. For $W = \hat{W}(I_1, I_2, J)$ we have,

$$\sigma_i = \frac{\lambda_i}{J} \left[\frac{\partial W}{\partial I_1} \frac{\partial I_1}{\partial \lambda_i} + \frac{\partial W}{\partial I_2} \frac{\partial I_2}{\partial \lambda_i} + \frac{\partial W}{\partial J} \frac{\partial J}{\partial \lambda_i} \right] \quad \text{(no sum on } i\text{)} \tag{A4}$$

or

$$\sigma_i = \frac{\lambda_i}{J}\left[\frac{\partial W}{\partial I_1}\frac{\partial I_1}{\partial \lambda_i} + \frac{\partial W}{\partial I_2}\frac{\partial I_2}{\partial \lambda_i}\right] + \frac{\partial W}{\partial J} \quad \text{(no sum on } i\text{)} \tag{A5}$$

The corresponding nominal stress (force per unit original area) is given by:

$$f_i = \frac{J}{\lambda_i}\sigma_i \quad \text{(no sum on } i\text{)} \tag{A6}$$